Journal of Macromolecular Science, Part A
Publication details, including instructions for authors and subscription information:
http://www.informaworld.com/smpp/title~content=t713597274

Synthesis and Characterization of Poly(methyl methacrylate-*co*-hydroxyethyl methacrylate)-*b*-polyisobutylene-*b*-poly(methyl methacrylate-*co*-hydroxyethyl Methacrylate) Triblock Copolymers

Dingsong Feng[a]; Amol Chandekar[a]; James E. Whitten[a]; Rudolf Faust[a]
[a] Polymer Science Program, Department of Chemistry, University of Massachusetts Lowell, Lowell, MA

To cite this Article Feng, Dingsong , Chandekar, Amol , Whitten, James E. and Faust, Rudolf(2007) 'Synthesis and Characterization of Poly(methyl methacrylate-*co*-hydroxyethyl methacrylate)-*b*-polyisobutylene-*b*-poly(methyl methacrylate-*co*-hydroxyethyl Methacrylate) Triblock Copolymers', Journal of Macromolecular Science, Part A, 44: 11, 1141 — 1150
To link to this Article: DOI: 10.1080/10601320701561015
URL: http://dx.doi.org/10.1080/10601320701561015

Journal of Macromolecular Science®, Part A: Pure and Applied Chemistry (2007) **44**, 1141–1150

ISSN: 1060-1325 print/1520-5738 online
DOI: 10.1080/10601320701561015

Synthesis and Characterization of Poly(methyl methacrylate-*co*-hydroxyethyl methacrylate)-*b*-polyisobutylene-*b*-poly(methyl methacrylate-*co*-hydroxyethyl Methacrylate) Triblock Copolymers

DINGSONG FENG, AMOL CHANDEKAR, JAMES E. WHITTEN, and RUDOLF FAUST
Polymer Science Program, Department of Chemistry, University of Massachusetts Lowell, Lowell, MA

Received and accepted June, 2007

The synthesis of poly[(methyl methacrylate-*co*-hydroxyethyl methacrylate)-*b*-isobutylene-*b*-(methyl methacrylate-*co*-hydroxyethyl methacrylate)] P(MMA-*co*-HEMA)-*b*-PIB-*b*-P(MMA-*co*-HEMA) triblock copolymers with different HEMA/MMA ratios has been accomplished by the combination of living cationic and anionic polymerizations. P(MMA-*co*-HEMA)-*b*-PIB-*b*-P(MMA-*co*-HEMA) triblock copolymers with different compositions were prepared by a synthetic methodology involving the transformation from living cationic to anionic polymerization. First, 1,1-diphenylethylene end-functionalized PIB (DPE-PIB-DPE) was prepared by the reaction of living difunctional PIB and 1,4-*bis*(1-phenylethenyl)benzene (PDDPE), followed by the methylation of the resulting diphenyl carbenium ion with dimethylzinc ($Zn(CH_3)_2$). The DPE ends were quantitatively metalated with *n*-butyllithium in tetrahydrofuran, and the resulting macroanion initiated the polymerization of methacrylates yielding triblock copolymers with high blocking efficiency. Microphase separation of the thus prepared triblock copolymers was evidenced by the two glass transitions at -64 and $+120^{\circ}C$ observed by differential scanning calorimetry. These new block copolymers exhibit typical stress-strain behavior of thermoplastic elastomers. Surface characterization of the samples was accomplished by angle-resolved X-ray photoelectron spectroscopy (XPS), which revealed that the surface is richer in PIB compared to the bulk. However, a substantial amount of P(MMA-*co*-HEMA) remains at the surface. The presence of hydroxyl functionality at the surface provides an opportunity for further modification.

Keywords: block copolymer; combination of polymerization mechanism; thermoplastic elastomers; surface characterization

1 Introduction

Living polymerization is the most efficient method for the synthesis of block copolymers since it allows precise control of molecular weights and molecular weight distributions. Well-defined ABA triblock copolymers consisting of a rubber center block and glassy or crystalline end blocks are widely used as thermoplastic elastomers (TPEs), where hard block domains are dispersed in the continuous rubbery matrix. TPEs exhibit properties similar to chemically cross-linked elastomers at room temperature, while at elevated temperatures they behave as thermoplastics.

Polyisobutylene (PIB) based TPEs have attracted considerable attention recently because of their unique properties such as biostability and biocompatibility due to the saturated backbone. For example, poly(styrene-*b*-isobutylene-*b*-styrene) (SIBS) triblock copolymer has been employed as a drug (paclitaxel, PTx) eluting coating for the TAXUS™ stent (Boston Scientific Corp.). PTx, however, is incompatible with SIBS, and PTx diffusion through SIBS is extremely slow. Recently, it was found that the polarity of the end blocks affects the drug-polymer miscibility and allows flexibility in tuning the drug release rate (1). Therefore, recent research efforts in our laboratory have focused on the synthesis of PIB based block copolymers containing polar end segments. For instance, replacing styrene in SIBS with acetoxystyrene resulted in an increased PTx release rate, while substitution with *p*-hydroxystyrene resulted in an initial burst release followed by a slower sustained release (2).

Triblock copolymers comprised of IB and polar monomers, such as methacrylates, combine the unique properties of PIB with the properties of polar polymers. They are also outstanding candidates as a polymer matrix for drug eluting stent coatings. IB can be polymerized only by cationic methods.

Address correspondence to: Rudolf Faust, Polymer Science Program, Department of Chemistry, University of Massachusetts Lowell, One University Avenue, Lowell, MA 01854. E-mail: rudolf_faust@uml.edu

Methacrylates do not undergo cationic polymerization; however, anionic polymerization provides well-defined poly(methacrylates) under selected conditions. Therefore, the combination of cationic and anionic polymerization is essential for the synthesis of well-defined block copolymers consisting of PIB and poly(methacrylate). A variety of methods have already been reported. For instance, Müller et al. reported the synthesis of PIB-*b*-poly(*t*butyl methacrylate) (P*t*BMA) and poly(methyl methacrylate) (PMMA)-*b*-PIB-*b*-PMMA by metalation of DPE end-capped PIB with Na/K alloy or cesium followed by anionic polymerization (3, 4). Another attempt demonstrated by Müller et al. involved the preparation of thiophene end-functionalized PIB and subsequent metalation of the polymer chain end with an alkyllithium compound, followed by polymerization of tBMA with the generated macroanion (5). In a recent publication, we also reported the synthesis of PIB-*b*-PMMA by a novel coupling approach combining living cationic and anionic polymerization techniques (6). Bromoallyl end-functionalized PIB (PIB-AllylBr) was coupled with living poly(-methyl methacrylate) anion in THF at -78°C to yield PIB-*b*-PMMA diblock copolymer with high coupling efficiency ($>95\%$).

For the synthesis of PMMA-*b*-PIB-*b*-PMMA and PHEMA-*b*-PIB-*b*-PHEMA block copolymers a novel site transformation technique from cationic to anionic polymerization has been recently developed (7). This method involved the preparation of DPE end-functionalized PIB (PIB-DPE), which could be quantitatively metalated with *n*-butyllithium (*n*-BuLi). The resulting macroanion efficiently initiated the living polymerization of methacrylate monomers at -78°C to afford the desired triblock copolymers. The PMMA-*b*-PIB-*b*-PMMA/PTx system exhibited a zero-order drug release that was somewhat faster than that from SIBS. A significant initial burst was observed, on the other hand, from PHEMA-*b*-PIB-*b*-PHEMA/PTx coatings. We hypothesized that a further optimization in drug delivery can be accomplished by synthesizing triblock copolymers containing P(HEMA-*co*-MMA) as glassy segments. Introduction of HEMA in the hard segment may offer an opportunity to modulate the drug release behavior and provide hydroxyl functionality for further modifications.

Surface modification methods have been widely used to improve blood/tissue compatibility. To modify polymer surfaces, one approach is to incorporate the surface-active end groups in the backbone of the polymers during synthesis. The presence of the hydroxyl functionality in these new triblock copolymers provides an opportunity to attach bioactive agents on surfaces of these copolymers films. To accomplish this, it is important to quantify the surface composition of the copolymer films. X-ray photoelectron spectroscopy (XPS) is an excellent technique to evaluate the surface composition of polymer films (8). It is well known that the surface composition of a polymer film may be considerably different from the bulk composition since low surface energy components tend to migrate to the surface to minimize the surface free energy. For example, Wen et al. reported significant enrichment of polydimethylsiloxane (PDMS) at the surface when PDMS was introduced to modify the soft segment of polyurethane (9).

The present paper reports the synthesis, characterization and properties of a series of P(MMA-*co*-HEMA)-*b*-PIB-*b*-P(MMA-*co*-HEMA) having varying composition, using 2-[(trimethylsilyl)oxy]ethyl methacrylate (TMSiOEMA) as a precursor of HEMA by the site transformation technique previously reported for anionic polymerization. Investigation of the surface composition of the polymer films by angle-resolved X-ray photoelectron spectroscopy at different depths is also reported.

2 Experimental

2.1 Materials

2-Chloro-2,4,4-trimethylpentane (TMPCl) and 5-tert-butyl-1,3-bis(1-chloro-1-methylethyl)benzene (*t*BuDiCumCl) were synthesized following the procedures reported elsewhere (10, 11). 1,4-*Bis*(1-phenylethenyl)benzene (PDDPE) was prepared by using the procedures analogous to those reported by Tung and Lo (12). 2,6-Di-*tert*-butylpyridine (DTBP, Aldrich, 97%), titanium tetrachloride ($TiCl_4$, Aldrich, 99.9%), dimethylzinc ($Zn(CH_3)_2$, Aldrich, 2.0 *M* in toluene), *n*-butyllithium (*n*-BuLi, Aldrich, 1.6 M in hexanes), triethylaluminum ($AlEt_3$, Aldrich, 25 wt% in toluene), benzoic anhydride (Aldrich, 97%), pyridine (Aldrich, 97%) and trioctylaluminum ($AlOct_3$, Aldrich, 25 wt% in hexanes) were used as received. The active concentration of *n*-BuLi solution was determined by polymerization of styrene. Purification of tetrahydrofuran (THF, Aldrich, 99+%), methyl methacrylate (MMA, Aldrich, 99%), 1,1-diphenylethylene (DPE, Aldrich, 97%), 2-[(trimethylsilyl)oxy]ethyl methacrylate (TMSiOEMA, Gelest, $>95\%$), hexanes (Hex), methyl chloride (MeCl), methylene chloride (CH_2Cl_2), and isobutylene (IB, Airgas) was carried out as described previously (7). The synthesis and purification of PIB-DPE and DPE-PIB-DPE have been described elsewhere (7, 13).

2.2 Copolymerization of MMA and TMSiOEMA

All polymerizations were carried out under high vacuum conditions ($<10^{-6}$ mbar) in THF at -78°C in a sealed glass reactor with break-seals. In a typical experiment, to a 100 mL round bottom flask equipped with break-seals were added DPE (0.081 g, 0.45 mmol) and *n*-BuLi (1.6 M $\times$ 0.6 mL $=$ 0.96 mmol) in hexanes using a dried gas tight syringe under argon. After evaporating hexanes completely under high vacuum, THF (50 mL) was added by trap-to-trap distillation over 1,1-diphenylhexyllithium (DPHLi) at -78°C. The solution was allowed to stand at -78°C for 10 min and then at 25°C for 2 h to decompose *n*-BuLi used

in excess. After degassing the solution at −78°C for 10 min and heat-sealing the apparatus off-line, an MMA/TMSiOEMA monomer mixture with predetermined molar ratio (25/75) in THF was added with vigorous stirring to start the polymerization. After 1 h, the living polymer was quenched with methanol (1 mL).

2.3 Synthesis of PIB-b-P(MMA-co-HEMA)

The polymerization was carried out in THF at −78°C under high vacuum ($<10^{-6}$ torr) in a sealed glass reactor with break-seals. In a typical experiment, THF (45 mL) was added to a 100 mL round bottom flask equipped with break-seals by trap-to-trap distillation over DPHLi at −78°C. After degassing the solution at −78°C for 10 min, the apparatus was cut off from the vacuum line by heat-sealing. 0.42 g of PIB-DPE (M_n 4,200, 0.1 mmol) dissolved in 5 mL of hexanes was then added. Dilute DPHLi solution was added dropwise to the reactor at room temperature until the color of the polymer solution turned to yellow, indicating there were no protic impurities in the polymer solution. Lithiation was performed by adding 1.5-fold excess *n*-BuLi (0.15 mmol) at room temperature for 10 min. Then, the polymer solution was cooled down to −78°C and MMA/TMSiOEMA monomer mixture with predetermined molar ratio (50/50) in THF was added with vigorous stirring to start the polymerization. After completion of the copolymerization of MMA/TMSiOEMA at −78°C in 1 h, a small portion of polymer solution was taken for GPC measurement. The rest of the polymer solution was quenched with 1 mL methanol. The solution was poured into a large amount of water to give a white solid polymer, which was dried by a freeze-dryer. The polymer was extracted with hexanes to remove deactivated PIB precursor at room temperature for 24 h.

2.4 Synthesis of P(MMA-co-HEMA)-b-PIB-b-P(MMA-co-HEMA)

The synthesis of triblock copolymer was carried out using DPE-PIB-DPE in a similar manner as that of PIB-*b*-P(MMA-*co*-HEMA). THF (120 mL) and hexanes (30 mL) were added to a 250 mL round bottom flask equipped with break-seals by trap-to-trap distillation over DPHLi at −78°C. After degassing the solution at −78°C for 10 min, the apparatus was cut off from the vacuum line by heat-sealing. 3.0 g of DPE-PIB-DPE (M_n 60,100, 0.05 mmol) dissolved in 20 mL of hexanes was then added. Dilute DPHLi solution was added dropwise to the reactor at room temperature until the color of the polymer solution turned yellow. Lithiation was performed by adding 1.5-fold *n*-BuLi (0.15 mmol) at room temperature for 10 min. The polymer solution was then cooled down to −78°C, and MMA/TMSiOEMA monomer mixture (molar ratio = 25/75) in THF was added with vigorous stirring to start the polymerization. After completion of the copolymerization of MMA/TMSiOEMA at −78°C in 1 h, the polymer solution was quenched with methanol (1 mL). The solution was poured into a large amount of water to give a white solid polymer, which was freeze-dried for 3 days. The polymer was purified by the extraction of deactivated PIB precursor with hexanes for 24 h and then with methanol to remove hydrolysis residue.

2.5 Benzoylation of PHEMA (14)

0.5 g of HEMA-containing polymer was dissolved in 6 mL of anhydrous pyridine. Under a nitrogen atmosphere, 4.5 g of benzoic anhydride was added slowly at 0°C. The reaction mixture was stirred at room temperature for 48 h. The reaction solution was then poured into a large amount of water for precipitation. The polymer was redissolved in THF and then precipitated into methanol twice.

2.6 Nuclear Magnetic Resonance

Nuclear Magnetic Resonance (NMR) spectroscopy was carried out on a Bruker 500 MHz spectrometer using $CDCl_3$ as a solvent. ^{1}H NMR spectra of solutions in $CDCl_3$ were calibrated with tetramethylsilane (TMS) as the internal standard (δ_H 0.00).

2.7 Molecular Weight Characterization

Molecular weights and molecular weight distributions of polymers were measured at room temperature using a Waters HPLC system equipped with a model 510 HPLC pump, model 410 differential refractometer, model 486 UV/visible detector, online multi-angle laser light scattering (MALLS) detector (MiniDawn, Wyatt Technology Inc.), model 712 sample processor, and five Waters ultraStyragel® columns connected in series (500, 10^3, 10^4, 10^5, and 100 Å). THF was used as an eluent at a flow rate of 1 mL/min.

2.8 Mechanical Properties

The tensile properties were measured on solution cast samples according to ASTM D638-02a. Solution cast samples were prepared by dissolving the polymer in THF (5 wt%). The polymer solution was poured into a teflon mold and the solvent was allowed to evaporate slowly for ~5 days at room temperature to avoid bubbles in the sample. The dried films were annealed at 130°C under vacuum for 24 h.

2.9 Differential Scanning Calorimetry (DSC)

The glass transition temperatures (T_gs) of the triblock copolymers were determined by a DuPont 910 differential scanning calorimeter calibrated with indium for onset temperature and enthalpy change. The samples were heated to 150°C at 20°C/min, held isothermal for 5 min, and then cooled to −100°C at 20°C/min. Thermograms were recorded during the second heating cycle from −100°C to 150°C at 20°C/min.

2.10 X-Ray Photoelectron Spectroscopy (XPS)

Surface analysis of the polymer films was performed with XPS using a Vacuum Generators ESCALAB MKII instrument under ultrahigh vacuum ($<10^{-9}$ Torr) using MgKα X-rays (1253.6 eV). The photoelectrons were energy-analyzed with a concentric hemispherical analyzer in fixed analyzer transmission mode using a pass energy of 20 eV. All specimens for surface analysis were prepared by spin coating from chloroform solutions (5 wt%) onto steel alloy disks. No corrections for surface charging (which results in the XPS peaks shifting to higher binding energies) have been made. To a first approximation, all peaks and peak components shift by the same amount due to this effect. Data processing and curve fitting were performed using Avantage software for surface chemical analysis.

XPS spectra were recorded at two different take-off angles (90° and 30°). Note that the take-off angle (TOA) has been defined in different ways; here it refers to the angle between the plane of the sample and the normal to the entrance of the electron energy analyzer. Detection depth depends on the TOA (θ) and the inelastic mean free path (λ) of the escaping photoelectrons, with 95% of the photoelectron signal originating from a depth of $3\lambda \sin\theta$ (ref. 8, page 36). C1s electrons ejected by MgKα X-rays have kinetic energy of ca. 970 eV, which corresponds to a mean free path (λ) of approximately 24 Å for electrons traversing through organic material (ref. 8, page 39). Therefore, for 90° and 30° TOAs, 95% of the XPS signal originates from less than ca. 7 and 4 nm, respectively. Note that this is an approximate depth since the mean free path is material dependent, with mean free path values in the range of 30 Å also commonly reported for organic films (15, 16).

3 Results and Discussions

PIB-DPE and DPE-PIB-DPE. Control of chain-end functionality is a key process for the site transformation technique. The detailed synthetic procedure of PIB-DPE was described in a previous paper (7). Figure 1 shows the ^{1}H-NMR spectra of the obtained PIB-DPE. The resonances at 7.42–7.20 and 5.48–5.43 ppm were assigned to protons on the phenyl ring and vinyl group after the capping reaction. The number average degree of polymerization can be obtained by the integration ratio of the signals for vinyl protons and the methylene protons in the PIB main chain. By using the ratio of M_n (GPC)/M_n (NMR), (4200/4000), the DPE functionality was quantitative within experimental error. The absence of resonances at 3.07 ppm, corresponding to the methoxy group, indicates complete methylation.

3.1 Anionic Copolymerization of MMA/TMSiOEMA

The reactivity of most methacrylic esters is independent of the nature of the alkoxy group, as has been shown for MMA/glycidyl methacrylates pair (17). Unfortunately, little information is available in the literature on the anionic copolymerization of MMA/TMSiOEMA. Ruckestein and Zhang reported the synthesis of P(MMA-*co*-HEMA) containing <15 wt% HEMA by anionic copolymerization of MMA/TMSiOEMA followed by hydrolysis, due to poor solubility of the resulting copolymer in THF (18). However, no detail was given on the monomer sequence distribution. The present study investigated the anionic copolymerization of MMA/TMSiOEMA at a wide composition range from 25–75 (mol)% MMA (Table 1). The bulky initiator was prepared *in situ* by reacting DPE with *n*-BuLi. Anionic copolymerization was performed at −78°C in THF by feeding a prechilled monomer mixture.

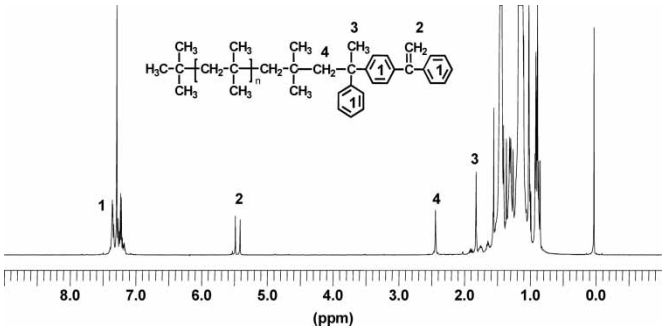

Fig. 1. ^{1}H-NMR spectrum of PIB-DPE.

During workup, the trimethylsilyl group was spontaneously cleaved to form HEMA. The visually complete hydrolysis is confirmed by a negligible amount of silane found by ^{1}H-NMR spectroscopy (Figure 2). Since PHEMA is insoluble in THF, to determine the molecular weight and molecular weight distribution by GPC in THF, the polymers were reacted with benzoic anhydride in pyridine to afford poly[2-(benzoyloxy)ethyl methacrylate], which is soluble in THF. Because of the living nature of copolymerization, the determined molecular weight is close to the calculated value and the molecular weight distribution is narrow. As shown in Figure 3, the GPC refractive index (RI) trace of a representative copolymer exhibited a single sharp peak. The yield of copolymers is quantitative in all cases. This is further confirmed by the agreement of the compositions in the comonomer mixture and in the

Table 1. Anionic copolymerization of HEMA and TMSiOEMA

MMA/TMSiOEMA (mol/mol)	M_n Calcd	M_n Obsd[a]	M_w/M_n[a]	W_{MMA}/W_{HEMA}[b]
74/26	13200	14700	1.08	68/32
48/52	9300	10200	1.10	44/56
25/75	11400	12900	1.12	20/80

[a]Determined by GPC before hydrolysis.
[b]Determined by ^{1}H-NMR of benzoylated samples.

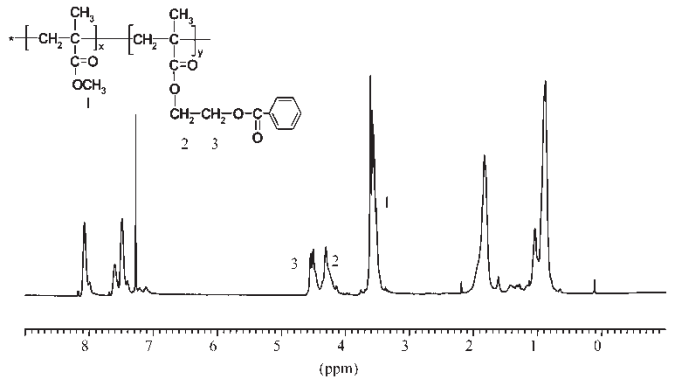

Fig. 2. ^{1}H-NMR spectrum of benzoylated P(MMA-*co*-HEMA).

copolymer determined by ^{1}H-NMR spectroscopy. In the ^{1}H-NMR spectrum (Figure 2) of a representative sample, the methoxy protons show broad and multiple peaks, suggesting random distribution of the comonomers. ^{13}C-NMR spectroscopy in the carbonyl region is usually used to investigate the tacticity of poly(methacrylates) (19). Figure 4 shows the ^{13}C-NMR spectra in the carbonyl region for PMMA, benzoylated PHEMA and benzoylated P(MMA-*co*-HEMA). The ^{13}C-NMR resonance was recorded in the region of 176–179 ppm with respect to the central peak of $CDCl_3$ at 77.2 ppm. Both PMMA and PHEMA prepared by anionic polymerization are highly syndiotactic. The broad peaks of P(MMA-*co*-BOEMA) indicate the loss of syndiotactic structure. Moreover, the carbonyl signals of benzoylated P(MMA-*co*-HEMA) appeared intermediate between the resonances of homopolymers. This observation further confirmed the randomness of the copolymerization.

3.2 Synthesis of PIB-b-P(MMA-co-HEMA)

The macroinitiator for anionic polymerization was obtained by the reaction of PIB-DPE with 1.5-fold *n*-BuLi, and then at -78°C the pre-chilled monomer mixture was fed to start anionic copolymerization (Scheme 1). To avoid termination of PIB macroanion by

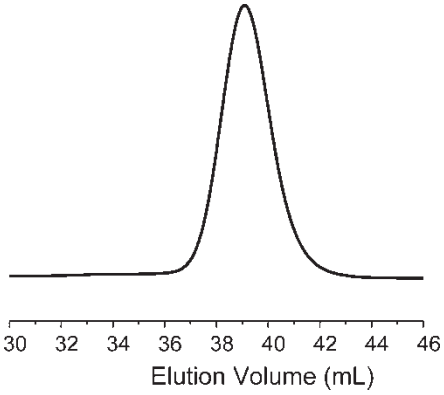

Fig. 3. GPC RI traces of P(MMA-*co*-HEMA) with MMA/HEMA mole ratio of 75/25 after benzoylation.

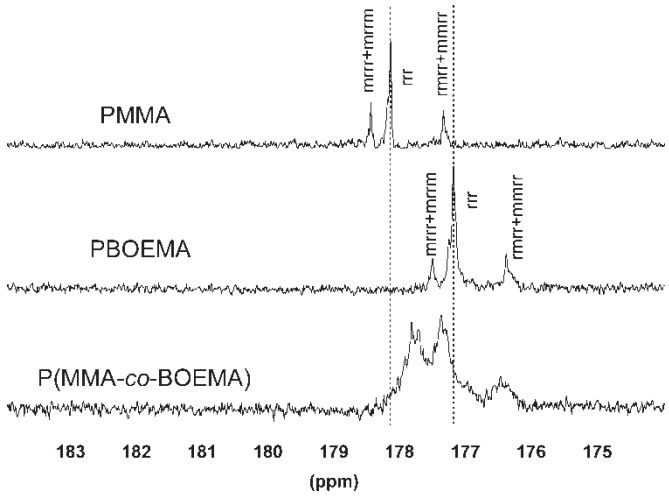

Fig. 4. ^{13}C-NMR spectra of carbonyl group at (A) PMMA, (B) benzoylated PHEMA and (C) benzoylated P(MMA-*co*-HEMA).

possible protic impurities present in the polymer, a dilute DPHLi solution was added drop-wise to the polymer solution until a light red color persisted before the lithiation. The application of DPHLi cleansing agent solution eliminated the need for a critical purification of the PIB-DPE precursor. Upon the addition of *n*-BuLi, a deep red color developed immediately, indicating the formation of PIB diphenyl carbanion. It has been shown that the lithiation of PIB-DPE is quantitative in 1 min (7). It is presumed that a slight excess *n*-BuLi ($<10^{-3}$ M) is decomposed by THF in 10 min at room temperature.

A small amount of polymer solution was taken out for GPC characterization before quenching the reaction with methanol. The GPC traces of the resulting polymer are bimodal. The peak in the low molecular region appears exactly at the same elution volume as the PIB precursor, corresponding to deactivated PIB (Figure 5). Since the UV detector only detects the aromatic group of PIB-DPE, the blocking efficiency (B_{eff}) can be calculated from the UV trace according to the following equation:

$$B_{eff} = A_{block}/(A_{PIB} + A_{block}) \times 100\%$$

where A_{block} is the peak area corresponding to the diblock copolymer, and A_{PIB} is the peak area corresponding to deactivated PIB precursor obtained by peak deconvolution.

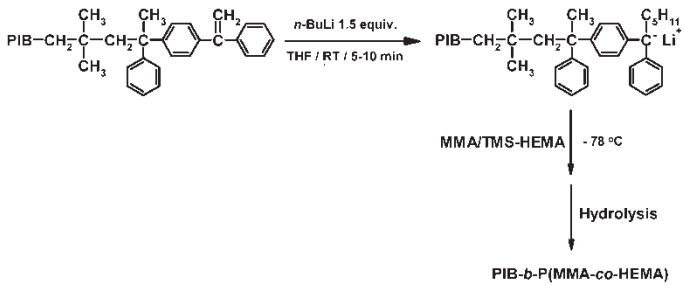

Sch. 1. Synthetic route of PIB-*b*-P(MMA-*co*-HEMA) copolymer.

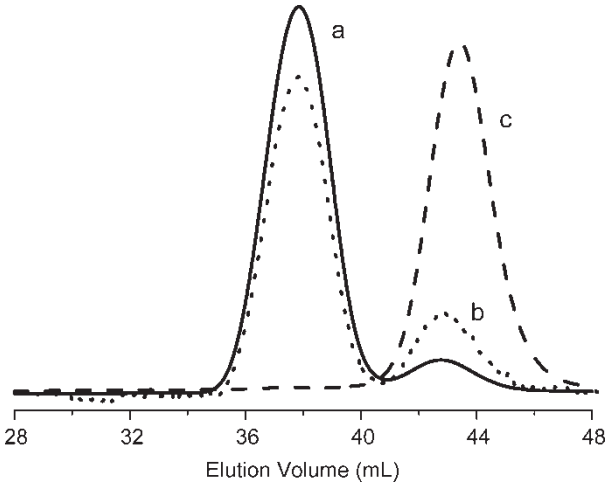

Fig. 5. GPC traces of PIB-DPE (M_n 4,200, M_w/M_n 1.08) and PIB-*b*-P(MMA-*co*-TMSiOEMA) diblock copolymer before hydrolysis. (a) RI trace of diblock copolymer; (b) UV trace of diblock copolymer; (c) RI trace of PIB-DPE.

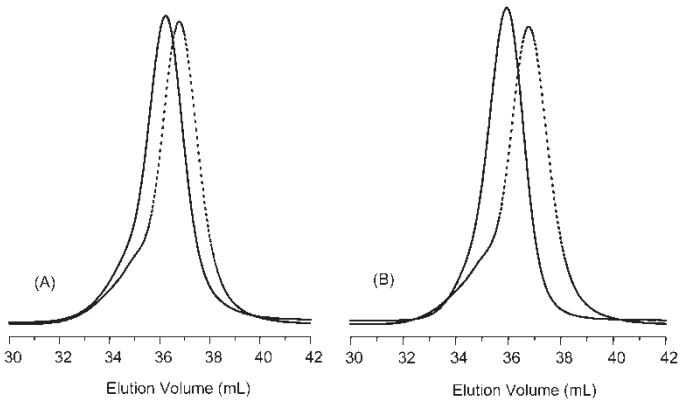

Fig. 6. GPC RI traces of DPE-PIB-DPE (dotted line) and the triblock copolymer (solid line) (A) ABA2 and (B) ABA5 after benzoylation.

Table 2 summarizes the blocking efficiencies at two different MMA/TMSiOEMA ratios. Representative samples were also analyzed by selective solvent extraction of deactivated PIB using hexanes. By comparing the mass of extracted PIB with the original amount of PIB precursor used, the blocking efficiency can also be calculated. The results agreed well with the blocking efficiencies calculated from the GPC UV traces. Since double bonds could not be detected in the ^{1}H-NMR spectrum of homoPIB extracted by hexanes, lithiation was quantitative. Therefore, the presence of homoPIB suggests that the PIB-DPE macroinitiator was deactivated during MMA polymerization.

3.3 Synthesis of P(MMA-co-HEMA)-b-PIB-b-P(MMA-co-HEMA)

DPE-PIB-DPE with high molecular weight was prepared using *t*BuDiCumCl as initiator (20). The capping agent PDDPE solution in CH_2Cl_2 was added into the living PIB solution. Because of a locally high concentration of living PIB, the obtained difunctional PIB precursor showed a small shoulder on the high molecular weight side (Figure 6, dotted line). The amount (~5 mole%) of coupled PIB precursor can be determined from deconvolution results of GPC UV traces since only the phenyl ring is detected by UV detector. Fortunately, this coupled PIB is still active for site transformation. As high molecular weight PIB is insoluble in THF at −78°C, a THF/Hex 70/30 (v/v) mixture was used for the triblock synthesis. First, the PIB precursor was titrated with a dilute DPHLi solution to remove protic impurities. The α,ω-dimacroanion for anionic polymerization was obtained by complete metalation of DPE-PIB-DPE with 1.5-fold excess *n*-BuLi at room temperature. The anionic copolymerization was performed at −78°C. The polymer solution was then poured into a large amount of water to isolate the polymer. A series of triblock copolymers containing PIB center blocks and end blocks with varying MMA/TMSiOEMA ratio were synthesized. The characterization of samples is summarized in Table 3.

Benzoylated samples were used to determine M_n and PDI for ABA4 and ABA5 by GPC since these samples were insoluble in THF. The molecular weights for ABA4 and ABA5, shown in Table 3, are calculated based on the composition and molecular weight of the benzoylated samples. Typical GPC traces are shown in Figure 6. As expected, the molecular weights are close to the theoretical value.

Samples ABA1, ABA2 and ABA3 were soluble in $CDCl_3$, however, ABA4 and ABA5 only swelled in $CDCl_3$. Therefore, the benzoylated samples of ABA4 and ABA5 were used for NMR characterization. Figure 7 shows the ^{1}H-NMR spectra of ABA2 and benzoylated ABA5. The methylene protons of HEMA units in ABA2 show resonances at 3.9 and 4.1 ppm. After benzoylation, the methylene protons of

Table 2. Blocking efficiencies (B_{eff}) of PIB-*b*-P(MMA-*co*-TMSiOEMA) copolymers

MMA/TMSiOEMA (mol/mol)	PIB-DPE		Block copolymer		B_{eff} (%)[b]	
	M_n	M_w/M_n	M_n	M_w/M_n	GPC UV	Extraction
75/25	4200	1.08	32,400	1.17	81	82
50/50	4200	1.08	34,800	1.11	84	86

[a]PIB block: M_n 4,200, M_w/M_n 1.08.
[b]Determined by the area of PIB precursor in the GPC UV trace (254 nm).

Table 3. P(MMA-*co*-HEMA)-*b*-PIB-*b*-P(MMA-*co*-HEMA) with different compositions

Samples	MMA/HEMA (mol/mol)	M_n	M_w/M_n	Composition (wt)[a] IB/MMA/HEMA	Deactivated PIB (%)[b]
ABA1	100/0	99,700	1.10	66.0/34.0/0	0.4
ABA2	75/25	110,800	1.21	55.5/29.8/14.7	2.2
ABA3	50/50	96,000	1.19	63.9/15.0/21.1	3.8
ABA4[c]	25/75	98,400	1.22	61.5/7.8/30.7	3.5
ABA5[c]	0/100	101,300	1.19	62.6/0/37.4	3.0

[a]Determined by ^{1}H-NMR.
[b]Hexanes soluble part.
[c]Based on NMR and GPC of the benzoylated polymer.

HEMA are slightly shifted to 4.1 and 4.3 ppm. The absence of the peak at 3.9 ppm verifies quantitative benzoylation. Peaks were not observed at 0.15 ppm, indicating quantitative hydrolysis of TMS:OEMA to HEMA. The composition of the triblock copolymer was calculated by comparing the integration value for methoxy protons in PMMA, pendant methylene protons in PHEMA and methylene protons of PIB.

The crude product was extracted with hexanes for 24 h to isolate deactivated PIB precursor from the block copolymer. According to ^{1}H-NMR measurements, the extracted polymer was homoPIB, and since vinyl protons were not detected, lithiation is quantitative.

3.4 Differential Scanning Calorimetry (DSC)

DSC is a useful technique to study phase separation in block copolymers with two immiscible segments. As shown in Figure 8, two T_g's are observed in the DSC thermograms for all five samples indicating phase separation. The T_g for the PIB segment is around −64°C, which is similar to that previously reported for poly(α-methylstyrene)-PIB-poly(α-methylstyrene) (21). The T_g for P(MMA-*co*-HEMA) was observed at around 120°C. However, the T_g for PHEMA block is higher than the one reported in the previous paper (7). The reason for this difference is unknown at present but may be due to the slightly different thermal history.

3.5 Stress-Strain Behavior

The tensile properties of the five samples with different MMA/HEMA ratios were measured on solution-cast films. The stress-strain curves are plotted in Figure 9, and the results are summarized in Table 4. All samples showed characteristic properties of TPEs.

The highest tensile strength for PIB-based TPEs may reach 24 MPa, the value reported for poly(styrene)-PIB-poly(styrene), hereafter referred to as PS-PIB-PS, and also for vulcanized butyl rubber (13, 22). It is known that a small amount of diblock contamination results in a rather large decrease in tensile strength. As reported by Morton (23) for PS-polybutadiene-PS and Hadjikyriacou et al. (24) for poly(α-methylstyrene)-PIB-poly(α-methylstyrene), 5% of diblock contamination decreases the tensile strength by ~30%. Therefore, the tensile strength listed in Table 4, ranging from 14.0 to 16.8 MPa, may indicate 5–10% diblock contamination.

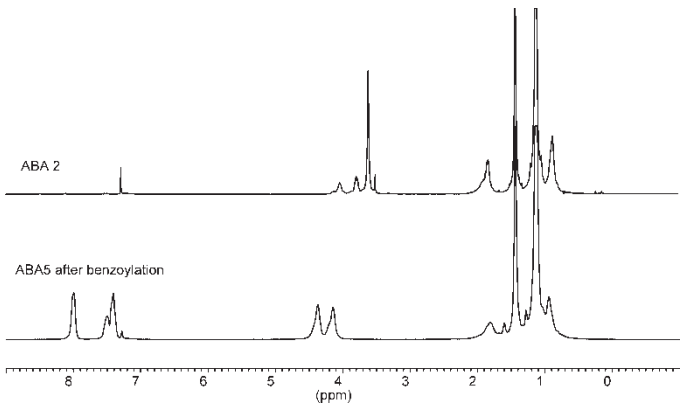

Fig. 7. ^{1}H-NMR characterization of triblock copolymers ABA2 and benzolated ABA5.

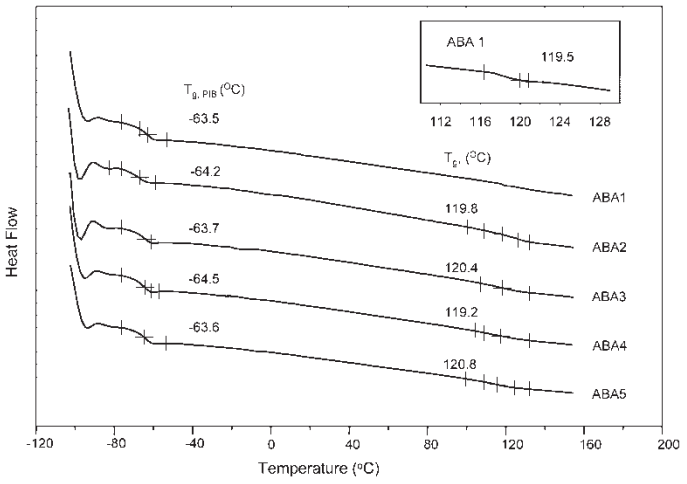

Fig. 8. DSC thermograms of P(MMA-*co*-HEMA)-*b*-PIB-*b*-P(MMA-*co*-HEMA) with different compositions.

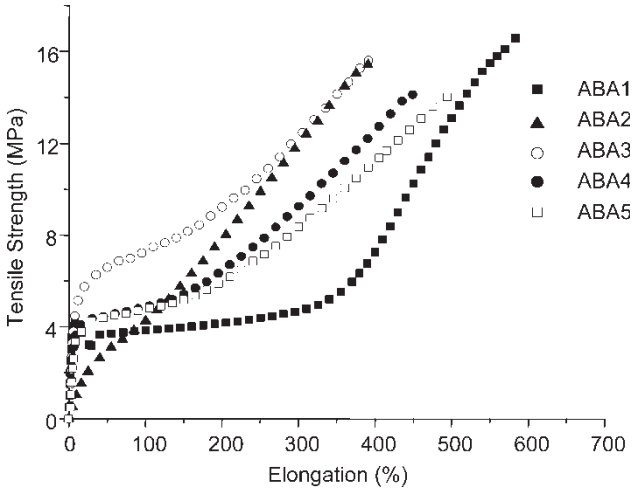

Fig. 9. Stress-strain plot for P(MMA-*co*-HEMA)-*b*-PIB-*b*-P(MMA-*co*-HEMA) triblock copolymer.

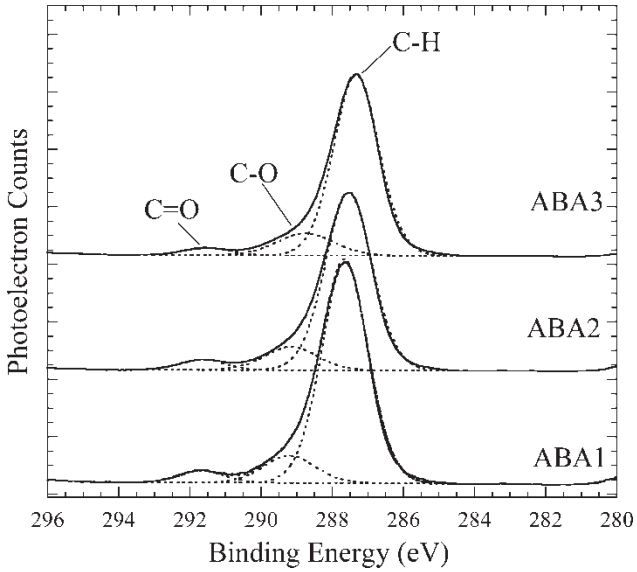

Fig. 10. Mgα C1s XPS spectra of ABA1, ABA2 and ABA3 polymer films acquired at a 90° TOA. The results of deconvoultion of the spectra into component peaks are shown as dashed lines. The locations of the C-H, C-O, and C═O component peaks are indicated. The spectra have not been corrected for surface charging.

3.6 Surface Composition

The surface elemental compositions of the copolymer films were calculated from the C1s and O1s XPS peak areas using appropriate sensitivity factors, and the results are summarized in Table 5. Figures 10 and 11 show C1s and O1s spectra, respectively, of polymers ABA1, ABA2 and ABA3 at a 90° take-off angle. These polymers differ in their MMA/HEMA molar ratios. Deconvolution of the C1s spectra indicates that there are three distinct peaks present corresponding to three different carbon species in the polymers. In increasing order of binding energy, these peaks may be assigned to carbon bonded to hydrogen (C-H), to carbon single-bonded to oxygen (C-O), and to carbon double-bonded to oxygen (C═O) at observed binding energies of 287.3, 288.8 and 291.5 eV, respectively. Because no corrections have been made for surface charging, these peaks appear at higher binding energies than those reported in the literature for PMMA and

Table 4. Mechanical properties of P(MMA-*co*-HEMA)-b-PIB-b-P(MMA-*co*-HEMA)

		M_n			
Samples	PIB%	PIB	P(MMA-*co*-HEMA)	Tensile strength (MPa)	Elongation (%)
ABA1	66.0	65100	17300	16.8	560
ABA2	55.5	60500	25100	15.6	390
ABA3	63.9	60500	17700	15.8	400
ABA4	61.5	60500	18900	14.2	450
ABA5	62.6	60500	20400	14.0	490

Table 5. Surface composition of ABA1, ABA2, and ABA3 films determined by XPS measurements

		C/O ratio		PIB wt%		
Code	TOA	Unannealed	Annealed[a]	Bulk	Unannealed	Annealed
ABA1	90°	93.3/6.7	95.8/4.2	66.0	76.1	84.9
	30°	95.8/4.2	96.3/3.7		85.1	86.9
ABA2	90°	91.5/8.5	95.6/4.4	55.5	71.4	85.1
	30°	93.6/6.4	96.1/3.9		78.4	86.8
ABA3	90°	91.4/8.6		63.9	72.0	
	30°	92.4/7.6			75.1	

[a]Annealing was performed at 130°C for 24 h.

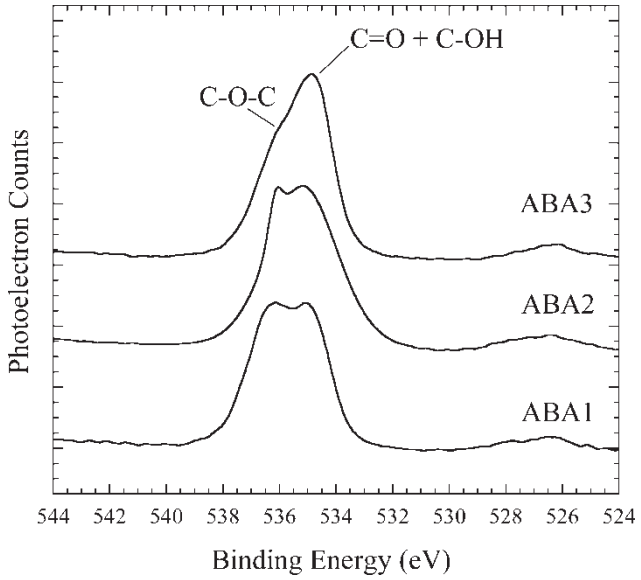

Fig. 11. MgKα O1s XPS spectra of ABA1, ABA2 and ABA3 polymer films acquired at a 90° TOA. As indicated, photoelectrons originating from C-O-C oxygen atoms appear at higher binding energy than those originating from C-O-H or C═O species. The spectra have not been corrected for surface charging.

PHEMA (25, 26). Correction (i.e., shifting) of the C-H peak to 285.0 eV would place the C-O and C═O peaks at 286.5 and 289.2 eV, respectively, in agreement with the literature. O1s spectra of these polymers show components at (uncorrected) binding energies of 534.9 and 536.4 eV. Correction for surface charging, by shifting the peaks the same amount to align the C-H peaks to 285.0 eV, would yield binding energies of 532.6 and 534.1 eV, respectively. In the case of ABA1, the lower binding energy component originates from the C═O oxygen species, while the higher binding energy one is due to the C-O-C group, consistent with the literature values (ref. 8, page 71). The known binding energy of C-OH oxygen atoms is ca. 532.9 eV (ref. 8, page 71), and the shapes of the O1s spectra for the three copolymers differ because of changes in the ratios of the peaks. For example, in the case of ABA1, the only source of oxygen is the PMMA blocks containing equal numbers of C-O-C and C═O groups, and a double-humped peak (with equal intensity in each hump) is observed. For ABA2, and even more so for ABA3, which contain C-O-H species in addition to C-O-C ones, the lower binding energy C═O and C-OH components dominate the C═O one.

XPS has been performed on PS-PIB-PS films (not shown) as a control experiment to determine the contribution of oxygen due to surface contamination. Only a trace amount of oxygen (<1 at.%) is detected, confirming that, in general, the polymer surfaces are virtually free from contamination. Also included in Table 5 are results of variable take-off angle studies performed to investigate surface segregation of the PIB block. Such studies are possible because PIB does not contain oxygen, in contrast to the MMA and HEMA blocks. Based on the measured C/O ratios, it is concluded from the more surface sensitive 30° TOA data that there is significant surface enrichment in PIB. This is expected since the surface tension of PIB (33.6 dyn/cm) is lower than that of PMMA (41.1 dyn/cm) and PHEMA (37.0 dyn/cm) (27). For all three samples, a composition gradient was observed. For example, ABA1 contains 66.0, 76.1 and 80.1 wt% PIB in the bulk, at 7 nm and at 4 nm detection depths, respectively. The bulk values are based on the known compositions of the polymers (from Table 3).

Figure 12 shows C1s spectra for ABA1 before and after annealing at two different take-off angles. After annealing, the higher binding energy peak due to C═O decreases in intensity relative to the main peak. This is consistent with attenuation of photoelectrons originating from the C═O groups present in PMMA due to blocking by surface PIB. This is due to PIB enrichment at the topmost surface of the polymer films after annealing; during annealing the free volume increases, and the PIB blocks with lower surface free energy diffuse to the surface. Quantitatively, the wt% of PIB at the surface (calculated based on the C/O atomic ratios) increases from 85 to 87% in the case of ABA1 and from 78 to 87% in the case of ABA2 after annealing. This surface enrichment in the PIB block may be due to slow segmental motion of the high molecular weight PIB segment ($M_{n,PIB} = 60.5$ k). In the case of ABA3, after annealing ca. 2% of Si accumulates at the surface, which is attributed to traces of hexamethyldisiloxane, a hydrolysis by-product. This makes it difficult to calculate the PIB content of the ABA3 film using C/O ratios since oxygen present in hexamethyldisiloxane complicates

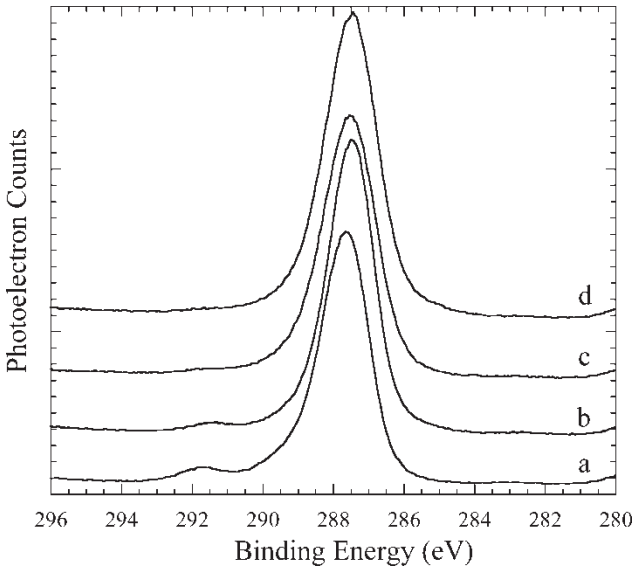

Fig. 12. MgKa C1s XPS spectra of the ABA1 polymer film at two different TOAs before and after annealing: a) 90° TOA before annealing, b) 30° TOA before annealing, c) 90° TOA after annealing, and d) 30° TOA after annealing. The spectra have not been corrected for surface charging.

the calculations. This annealing study shows that although surfaces of all three triblock copolymer films are rich in PIB, there is a considerable amount PMMA/P(MMA-*co*-HEMA) still present at the surfaces which has the hydroxyl functionality. Therefore, this study confirms that these block copolymer surfaces have the functionality required for subsequent surface modification.

4 Conclusions

The synthesis of PIB-*b*-P(MMA-*co*-HEMA) diblock and P(MMA-*co*-HEMA)-*b*-PIB-*b*-P(MMA-*co*-HEMA) triblock copolymers with varied MMA/HEMA compositions could be accomplished by site transformation from living cationic to anionic polymerization. All triblock copolymers exhibit thermoplastic elastomeric properties. The introduction of HEMA units in the hard segment may provide an opportunity to modulate the drug release behavior. In addition, XPS has shown that the hydroxyl functionalities are present on surfaces of the polymer films even after annealing, which provide an opportunity for further surface modification. Research on attaching bioactive agents to these new triblock copolymers is in progress.

5 Acknowledgment

Financial support by Boston Scientific Corp. is gratefully acknowledged.

6 References

1. Sipos, L., Som, A., Faust, R., Richard, R., Schwarz, M., Ranade, S., Boden, M. and Chan, K. (2005) *PMSE Prep.*, **92**, 41–42.
2. Sipos, L., Som, A., Faust, R., Richard, R., Schwarz, M., Ranade, S., Boden, M. and Chan, K. (2005) *Biomacromolecules*, **6(5)**, 2570–2582.
3. Feldthusen, J., Ivan, B. and Müller, A.H.E. (1997) *Macromolecules*, **30(22)**, 6989–6993.
4. Feldthusen, J., Iván, B. and Müller, A.H.E. (1998) *Macromolecules*, **31(3)**, 578–585.
5. Matinez-Castro, N., Lanzendolfer, M.G., Müller, A.H.E., Cho, J.C., Acar, M.H. and Faust, R. (2003) *Macromolecules*, **36(19)**, 6985–6994.
6. Higashihara, T., Feng, D. and Faust, R. (2006) *Macromolecules*, **39(16)**, 5275–5279.
7. Cho, J.C., Cheng, G., Feng, D., Faust, R., Richard, R., Schwarz, M., Chan, K. and Boden, M. (2006) *Biomacromolecules*, **7(11)**, 2997–3007.
8. Briggs, D. *Surface Analysis of Polymers by XPS and Static SIMS*; Cambridge University Press: Cambridge, 1998.
9. Wen, J., Somorjai, G., Lim, F. and Ward, R. (1997) *Macromolecules*, **30(23)**, 7206–7213.
10. Hadjikyriacou, S. and Faust, R. (1996) *Macromolecules*, **29(16)**, 5261–5267.
11. Gyor, M., Wang, H.C. and Faust, R. (1992) *J. Macromol. Sci., Pure Appl. Chem.*, **A29(8)**, 639–653.
12. Tung, L.H. and Lo, G.Y.S. U.S. Patent 4,182,818, 1980.
13. Fodor, Zs. and Faust, R. (1994) *J. Macromol. Sci., Pure Appl. Chem.*, **A31(12)**, 1985–2000.
14. Hirao, A., Kato, H., Yahoguchi, K. and Nakahama, S. (1986) *Macromolecules*, **19(5)**, 1294–1299.
15. Kondo, T., Yanagida, M., Shimazu, K. and Uosaki, K. (1998) *Langmuir*, **14(19)**, 5656–5658.
16. Lesiak, B., Kosinski, A., Jablonski, A., Kövér, L., Tóth, J., Varga, D., Cserny, I., Zagorska, M., Kulszewicz-Bajer, I. and Gergely, G. (2001) *Appl. Surf. Sci.*, **174(1)**, 70–85.
17. Hild, G., Lamps, Ph. and Rempp, P. (1993) *Polymer*, **34(13)**, 2875–2882.
18. Ruckenstein, E. and Zhang, H. (2000) *J. Polym. Sci.: Part A: Polym. Chem.*, **39(1)**, 117–126.
19. Yu, J., Dubois, P. and Jerome, R. (1997) *Macromolecules*, **30(21)**, 6536–6543.
20. Bae, Y.C. and Faust, R. (1998) *Macromolecules*, **31(26)**, 9379–9383.
21. Li, D. and Faust, R. (1995) *Macromolecules*, **28(14)**, 4893–4898.
22. Gyor, M., Fodor, Zs., Wang, H.-C. and Faust, R. (1994) *J. Macromol. Sci., Pure Appl. Chem.*, **A31(12)**, 2055–2065.
23. Morton, M. *Encyclopedia of Polymer Science and Technology*; Wiley: New York, Vol. 15, p.528, 1971.
24. Hadjikyriacou, S., Li, D., Bae, Y.C. and Faust, R. (1996) Macromolecular Symposia **107** (International Symposium on Ionic Polymerization, 1995), 65–74.
25. McArthur, S.L., McLean, K.M., St. John, H.A.W. and Griesser, H.J. (2001) *Biomaterials*, **22(24)**, 3295–3304.
26. Cossement, D., Gouttebaron, R., Cornet, V., Vivile, P., Hecq, M. and Lazzaroni, R. (2006) *Appl. Surf. Sci.*, **252(19)**, 6636–6639.
27. Wu, S. In *Polymer Handbook*, 4th Edn.; Brandrup, J., Immergut, E.H., Grulke, E.A., Abe, A. and Bloch, D.R. (Eds.); Wiley: New York, p.III/522, 1971.